Original Article

XB130 Knockdown Inhibits the Proliferation, Invasiveness, and Metastasis of Hepatocellular Carcinoma Cells and Sensitizes them to TRAIL-Induced Apoptosis

Guang-Ming Li[1], Chao-Jie Liang[2], Dong-Xin Zhang[1], Li-Jun Zhang[1], Ji-Xiang Wu[1], Ying-Chen Xu[1]

[1]Department of General Surgery, Beijing Tongren Hospital, Capital Medical University, Beijing 100730, China
[2]Department of General Surgery, First Hospital/First Clinical Medical College of Shanxi Medical University, Taiyuan, Shanxi 030001, China

Guang-Ming Li and Chao-Jie Liang contributed equally to this work.

Abstract

Background: XB130 is a recently discovered adaptor protein that is highly expressed in many malignant tumors, but few studies have investigated its role in hepatocellular carcinoma (HCC). Therefore, this study explored the relationship between this protein and liver cancer and investigated its molecular mechanism of action.

Methods: The expression of XB130 between HCC tissues and adjacent nontumor tissues was compared by real-time polymerase chain reaction, immunochemistry, and Western blotting. *XB130* silencing was performed using small hairpin RNA. The effect of silencing *XB130* was examined using Cell Counting Kit-8, colony assay, wound healing assay, and cell cycle analysis.

Results: We found that XB130 was highly expressed in HCC tissues (cancer tissues vs. adjacent tissues: 0.23 ± 0.02 vs. 0.17 ± 0.02, $P < 0.05$) and liver cancer cell lines, particularly MHCC97H and HepG2 (MHCC97H and HepG2 vs. normal liver cell line LO-2: 2.35 ± 0.26 and 2.04 ± 0.04 vs. 1.00 ± 0.04, respectively, all $P < 0.05$). The Cell Counting Kit-8 assay, colony formation assay, and xenograft model in nude mice showed that silencing *XB130* inhibited cell proliferative ability both *in vivo* and *in vitro*, with flow cytometry demonstrating that the cells were arrested in the G0/G1 phase in HepG2 (HepG2 *XB130*-silenced group [shA] vs. HepG2 scramble group [NA]: 74.32 ± 5.86% vs. 60.21 ± 3.07%, $P < 0.05$) and that the number of G2/M phase cells was decreased (HepG2 shA vs. HepG2 NA: 8.06 ± 2.41% vs. 18.36 ± 4.42%, $P < 0.05$). Furthermore, the cell invasion and migration abilities were impaired, and the levels of the epithelial-mesenchymal transition-related indicators vimentin and N-cadherin were decreased, although the level of E-cadherin was increased after silencing *XB130*. Western blotting showed that the levels of phosphorylated phosphoinositide 3-kinase (PI3K) and phospho-protein kinase B (p-Akt) also increased, although the level of phosphorylated phosphatase and tensin homolog increased, indicating that XB130 activated the PI3K/Akt pathway. Furthermore, we found that a reduction in XB130 increased liver cancer cell sensitivity to tumor necrosis factor-related apoptosis-inducing ligand-induced apoptosis.

Conclusions: Our findings suggest that XB130 might be used as a predictor of liver cancer as well as one of the targets for its treatment.

Key words: Apoptosis; Hepatocellular Carcinoma; PI3K/Akt; TRAIL; XB130

Introduction

Liver cancer is one of the most common malignancies in the world; owing to its high fatality and recurrence, it is mainly treated through surgery, radiation, and chemotherapy.[1] The advancement of science, technology, and medicine has slightly improved the early prognosis of liver cancer, but it remains the world's fifth highest cause of cancer-related death. Because the early stages of

Access this article online

Quick Response Code:

Website: www.cmj.org

DOI: 10.4103/0366-6999.241800

Address for correspondence: Dr. Ying-Chen Xu, Department of General Surgery, Beijing Tongren Hospital, Capital Medical University, Beijing 100730, China
E-Mail: xuyingchen66@163.com

Received: 25-04-2018 **Edited by:** Qiang Shi
How to cite this article: Li GM, Liang CJ, Zhang DX, Zhang LJ, Wu JX, Xu YC. *XB130* Knockdown Inhibits the Proliferation, Invasiveness, and Metastasis of Hepatocellular Carcinoma Cells and Sensitizes them to TRAIL-Induced Apoptosis. Chin Med J 2018;131:2320-31.

liver cancer tend to go undetected, it is usually diagnosed at the mid to late stage, reducing survival time.[2,3] Consequently, determining ways in which early diagnosis and treatment of liver cancer can be achieved has become an urgent issue,[4] resulting in the development of new cancer target predictions and therapies becoming a hot research topic.

Adaptor proteins are particular combinations of protein components that comprise multiple modules but lack an enzyme activity domain. They can participate in the regulation of various signaling pathways,[5] including those related to actin filament-associated protein (AFAP), Src-interacting or signal-integrating protein (Sin), and CRK-associated substrate. Studies have confirmed that c-Src activated by binding to the SH3 and SH2 domains[6,7] leads to the propagation of signals downstream; participates in signaling pathways; and regulates mitosis, validation, cell survival, movement, and adhesion.[8-10]

AFAP is a small adaptor protein that can participate in intracellular signal transduction, cytoskeletal structure, and other cellular functions that directly activate c-Scr and induce its activity by modulating mechanical distraction. In the process of cloning human AFAP, Lodyga *et al*.[11] discovered a novel adaptor protein named AFAP1L-2 on chromosome 10q25.3, which encodes an 818 amino acid protein with a molecular weight of 130,000 known as XB130. Since then, studies have shown that XB130 is a substrate and regulator of tyrosine kinase-mediated signal transduction and can bind with other tyrosine kinases via the SH2 and SH3 domains located in the N-terminal region of Src to phosphorylate tyrosine.[12]

It has been shown that the newly described adaptor protein XB130 plays a critical role in the regulation of signal transduction, which affects cell proliferation, survival, invasion, metastasis, and apoptosis.[13-16] Furthermore, XB130 is associated with the development of tumors,[17] being highly expressed in esophageal cancer,[14] gastric cancer,[18] and prostate cancer.[15] Some studies[14,15] have also found a relationship between the level of XB130 and the tumor classification, lymph node metastasis, TNM stage, and prognosis, but this differs between types of cancer. For instance, XB130 has been identified as a cancer-promoting protein in prostate cancer, with high levels predicting a poor prognosis, whereas the reverse is true for gastric cancer. Zuo *et al*.[19] found that XB130 is highly expressed in liver cancer, with a positive expression rate of 75%, but they did not report a comparison between cancer tissues and adjacent nontumor tissues or explore the molecular mechanism of XB130.

Therefore, this study explored the relationship between XB130 and liver cancer, the effect of reducing XB130 on hepatocellular carcinoma (HCC), and the molecular mechanism of action of XB130 to assess the possibility of using this protein as a target for the treatment of HCC.

Methods

Ethical approval

The experimental procedures were approved by the Beijing Tongren Hospital Research Ethics Committee. All applicable international, national, and/or institutional guidelines for the care and use of animals were followed. All procedures performed in studies involving human participants were in accordance with the ethical standards of the institutional and/or national research committee and with the 1964 *Declaration of Helsinki* and its later amendments or comparable ethical standards.

Tissue samples, cell lines, and reagents

Tumor tissues and adjacent tissues were obtained from twenty patients who were histologically diagnosed with liver cancer between October 2014 and February 2015. The human HCC cell lines HepG2, Bel-7402, and Huh-7 were obtained from the Cell Bank of Shanghai Institute of Biochemistry and Cell Biology (Shanghai, China). MHCC97H and SMCC7721 were purchased from the Bank of Zhongshan Hospital, Fudan University (Shanghai, China). Hep3B and the normal liver cell line LO-2 were received from the Cancer Hospital of the Chinese Academy of Medical Sciences (Beijing, China). Cells were cultured in Dulbecco's modified Eagle's medium supplemented with 10% fetal bovine serum (Gibco, Waltham, MA, USA), 100 U/ml penicillin, and 100 μg/ml streptomycin (Invitrogen, Carlsbad, CA, USA) in 5% CO_2 at 37°C. Cells were harvested in the logarithmic growth phase for use in the following experiments.

Mouse antibodies for vimentin, E-cadherin, N-cadherin, and XB130 were purchased from Santa Cruz Biotechnology Company (Santa Cruz, CA, USA). Rabbit antibodies for protein kinase B (Akt), Ser-473, Thr308, phoinositide 3-kinase (PI3K) P85, phosphatase P85, phosphatase and tensin homolog (PTEN), and p-PTEN were purchased from Cell Signaling Technology Company (Boston, MA, USA); glyceraldehyde-3-phosphate dehydrogenase (GAPHD) was obtained from Abcam (Shanghai, China), and a rabbit antibody targeting XB130 was obtained from PradoWalnut Company (Walnut, CA, USA). Ac-DEVD-AMC, Ac-IETD-AFC, and Ac-LEHD-AMC were purchased from BD Biosciences, San José, CA, USA.

Immunohistochemistry and evaluation of staining

IHC was performed with the anti-XB130 antibody. After isolation and hydration, the antigen was first recovered with citrate buffer (pH 6.0), following which the endogenous peroxidase activity was quenched with 0.3% hydrogen peroxide solution, and the sections were incubated with primary antibody (anti-XB130, 1:100) at room temperature for 2 h. The 3,3'-diaminobenzidine was used as a substrate to detect the binding of the antibody with the second antibody after incubation for 30 min at room temperature. Normal rabbit IgG was used as a negative control. Evaluation of staining was according to the description reported by Zuo *et al*.[19]

Lentiviral small hairpin RNA-mediated *XB130* silencing

XB130 silencing was performed using small hairpin RNA (shRNA). The sequences were shA (GCTGAAGATCACACCGATG), shB (GCCGATAGGGTCTCCTGTATT), and shC (GCTGAAGATCACACCGATG) for *XB130*-silencing shRNA and GCCAGCTTAGCACTGACTC for scramble shRNA.

Target shXB130 was cloned into the pLKO.1.-CMV vector. Target and nontarget vectors were packaged into lentiviral particles by BIOREE, Beijing, China. Each particle was transduced into appropriate human liver cancer lines and selected based on the antibiotic resistance. Clones were screened using Western blotting for XB130 expression.

Fluorescence quantitative real-time polymerase chain reaction

The primer sequences for human *XB130* were (F) 5′-AAG CAGCAGCTCTGATGAGG-3′ and (R) 5′-GGTCTGG AAGGCTCTTCTGA-3′. Total RNA was extracted from the cultured cells or tissues using the TRIzol® Kit (Life Technologies, Carlsbad, CA, USA). cDNA was then synthesized using total RNA and Moloney murine leukemia virus reverse transcriptase (MMLV-RT; Promega, Beijing, China). The reaction mixture for real-time polymerase chain reaction (RT-PCR) was prepared according to the manufacturer's protocol (BIORAD, Beijing, China).

Western blotting

The cells were lysed on ice in radioimmunoprecipitation assay buffer (50 mmol/L Tris-Cl [pH 7.5], 120 mmol/L NaCl, 10 mmol/L NaF, 10 mmol/L sodium pyrophosphate, 2 mmol/L ethylenediaminetetraacetic acid, 1 mmol/L Na_3VO_4, 1 mmol/L phenylmethylsulfonyl fluoride, and 1% NP-40) containing a protease inhibitor cocktail (Roche, Basel, Switzerland). The protein content of the lysates was determined by the bicinchoninic acid assay. First, 30 μg protein was separated by 8% or 12% sodium dodecyl sulfate-polyacrylamide gel electrophoresis and transferred to a nitrocellulose membrane (Millipore, Bedford, MA, USA). The membrane was then blocked in Tris-buffered saline and Tween 20 (TBST: 25 mmol/L Tris-HCl [pH 7.5], 125 mmol/L NaCl, and 0.1% Tween 20) containing 5% bovine serum albumin (BSA) and incubated with antibodies targeting XB130, E-cadherin, N-cadherin, vimentin, Akt, Ser473, Thr308, PTEN, p-PTEN, phos-PI3K (p-PI3K), PI3K, or GAPHD in TBST containing 1% BSA at 4°C overnight. Following this, the membrane was incubated with a suitable secondary antibody for 1 h at room temperature. Finally, immunoreactive protein bands were determined using the enhanced chemiluminescence system (Thermo Fisher Scientific, Waltham, MA, USA) and quantified using QuantityOne v4.6.2 imaging software (Bio-Rad, Hercules, CA, USA).

Viability assay

For the Cell Counting Kit-8 (CCK-8) assay, 5×10^3 cells were seeded in 96-well plates and observed for viability over 5 days. Cell viability was detected according to the manufacturer's instructions by measuring the absorbance at 450 nm through a microplate reader. Four replicate wells were used for each group.

Colony formation assay

For the colony formation assay, 100 individual cells from each group were seeded in six-well plates, cultured in 5% CO_2 at 37°C for 14 days, and stained with Giemsa stain. Colonies containing >50 cells were counted, and the efficiency was calculated as a percentage of inoculated cells.

Cell cycle analysis

Cells were fixed overnight at −20°C in 75% ethanol. The washed, precipitated cells were then resuspended in PBS containing 0.1% RNaseA (Fermentas) and 100 μl of 10 μg/ml propidium iodide (PI) (Sigma) for 30 min at room temperature. They were then subjected to flow cytometry using a FACScan (BD Biosciences), as previously described.

Analysis of apoptotic cells

Cells were harvested and stained with fluorescein isothiocyanate (FITC)-conjugated annexin V and PI according to the manufacturer's protocols using the annexin V-FITC/PI Kit (Cwbiotech, Beijing, China) and passed through a Cytomics FC500 flow cytometry system. Apoptotic changes were detected by FITC-conjugated annexin V staining, although PI was used to discriminate between apoptotic and necrotic cells among the annexin V-positive cells.

Wound healing assay

Cells were seeded into six-well plates at 90% confluence and incubated overnight to adherence. A wound was then made along the center of each well by scratching the cell layer with the tip of a 200-μl pipette. Next, the wells were washed twice with PBS to remove any loose cells, and fresh medium was added. Photographs were taken at 0 and 24 h to assess cell migration into the wound.

Transwell invasion assay

The invasive potential of wild-type and *XB130*-silenced germinal center cells was assessed using an invasion assay through a 24-well Matrigel Invasion Chamber (BD Biosciences, San José, CA, USA). A total of 5×10^4 cells per ml in 0.5 ml of serum-free medium were added to the upper chamber, and 0.75 ml of medium supplemented with 5% fetal bovine serum was added to each lower chamber. After 18 h of incubation, the invasive cells in the lower chamber were fixed with 3.7% paraformaldehyde, and the cells remaining in the upper chamber were removed by scratching. The cells were then washed twice with PBS, stained with hematoxylin at room temperature for 1 h, and photographed under a microscope.

Xenograft model in nude mice

BALB/c nude mice of 6 weeks old were purchased from Charles River Laboratories (Beijing, China). All laboratory procedures involving animals were based on the guidelines for the care and use of laboratory animals and were in line

with the ethical guidelines of our animal experiments. ShXB130-transfected and empty plasmid-transfected cells were trypsinized by centrifugation and suspended in Roswell Park Memorial Institute 1640 medium. Then, 0.2 ml of medium containing 1×10^7 cells was subcutaneously injected into the right posterior flank region of each mouse, following which the mice were incubated in a pathogen-free environment, and tumor growth was monitored every 4 days. The mice were sacrificed after 28 days, and the volume of each tumor was calculated according to the formula $V = a \times b \times (a + b)/2$, where "a" was the length and "b" was the width of the tumor measured with a sliding caliper.

Caspase assays

The substrates Ac-DEVD-AMC, Ac-IETD-AFC, and Ac-LEHD-AMC were used to assess the activities of caspase-3, caspase-8, and caspase-9 in protein extractions using fluorimeter according to the manufacturer's instructions (BD Biosciences, San José, CA, USA).

Statistical analysis

Each treatment was replicated in three separate experiments, and all data are expressed as mean ± standard deviation (SD). In all groups, comparisons were made using one-way analysis of variance (ANOVA). All statistical analyses were performed using Graphpad Prism 6.0 (Graphpad Software, La Jolla, CA, USA), and differences were considered statistically significant at $P < 0.05$.

Results

XB130 expression in hepatocellular carcinoma tissues and cell lines

To explore the relationship between HCC and XB130, we compared the expression of *XB130* between HCC tissues and adjacent nontumor tissues by RT-PCR and immunochemistry, wherein RT-PCR [Figure 1a] showed that the expression was significantly higher in HCC tissues compared with that in adjacent nontumor tissues (cancer tissues vs. adjacent tissues: 0.23 ± 0.02 vs. 0.17 ± 0.02, $P < 0.05$), and immunochemistry [Figure 1b] showed that the case number of positive expression of XB130 in cancer tissue was 16, the positive rate was 80%, and in adjacent tissues was 5, the positive rate was 25%; thus, the expression of XB130 in cancer tissues was significantly higher than that in adjacent tissues ($\chi^2 = 12.13$, $P < 0.01$). We then used RT-PCR and Western blotting to detect the expression of XB130 in the HCC cell lines HepG2, BEL-7402, Huh-7, Hep3B, SMCC7721, and MHCC97H and in the normal liver cell line LO-2. We found that the expression of XB130 was higher in HCC cell lines than that in normal liver cell lines (all $P < 0.05$), except Hep 3B. Because MHCC97H and HepG2 exhibited the highest expression [Figure 1c-1e], we used these cell lines for further research.

Silencing *XB130* inhibits proliferation of hepatocellular carcinoma cell lines

The expression of XB130 was lower in sh-MHCC97H and sh-HepG2 groups than that in scramble shRNA-transfected groups when we used shA, shB, shC, and scramble shRNA to transfect the cells, with the shA group exhibiting the lowest expression [Figure 2a and 2b] (HepG2: shA, shB, and shC vs. NC: 19.21 ± 3.12, 31.33 ± 9.93, and 28.35 ± 4.26 vs. 100.00 ± 7.69, $P < 0.01$; MHCC97H: shA, shB, and shC vs. NC: 16.18 ± 2.84, 34.47 ± 5.32, and 30.08 ± 10.78 vs. 100.00 ± 6.01, $P < 0.01$). Therefore, we selected shA as the research target and constructed stable silenced cell lines (MHCC97H shA and HepG2 shA). The scramble groups were used as control and named MHCC97H NC and HepG2 NC. To explore the effect of *XB130* knockdown on the proliferation of HCC cell lines, we analyzed cell proliferation using the CCK-8 assay and colony formation assay, as shown in Figure 2c-2e. The CCK-8 assay showed that MHCC97H shA and HepG2 shA groups had a significantly lower proliferative ability than the scramble groups (HepG2 shA vs. HepG2 NC: 1.26 ± 0.14 vs. 2.09 ± 0.14, $P < 0.05$; MHCC97H shA vs. MHCC97H NC: 1.35 ± 0.12 vs. 1.99 ± 0.10, $P < 0.05$). Furthermore, the number of clones formed was significantly reduced after silencing *XB130* (HepG2 shA vs. HepG2 NC: 1.26 ± 0.14 vs. 2.09 ± 0.14, $P < 0.05$; MHCC97H shA vs. MHCC97H NC: 1.35 ± 0.12 vs. 1.99 ± 0.10, $P < 0.05$). Flow cytometry showed that the number of G0/G1 phase cells increased in HepG2 shA compared with those in HepG2 NC (HepG2 shA vs. HepG2 NA: 74.32 ± 5.86% vs. 60.21 ± 3.07%, $P < 0.05$) and that the number of G2/M phase cells decreased following a reduction in XB130 both in HepG2 shA and MHCC97H shA groups (HepG2 shA vs. HepG2 NA: 8.06 ± 2.41% vs. 18.36 ± 4.42%, $P < 0.05$; Figures 2f and 2g]. Thus, the proliferation of MHCC97H and HepG2 cells decreased after silencing *XB130*.

Silencing *XB130* inhibits the motility and invasiveness of hepatocellular carcinoma cell lines and alters epithelial-mesenchymal transition markers

Next, we evaluated the effect of silencing *XB130* on the invasiveness and metastasis of HCC cell lines using a Transwell assay and wound healing assay [Figure 3a-3d], which showed that HepG2 shA and MHCC97H shA groups had significantly lower invasion and metastasis abilities than the NC groups (Transwell assay: HepG2 shA vs. HepG2 NC: 33.3 ± 5.2 vs. 207.0 ± 22.7, $P < 0.05$; Transwell assay: MHCC97H shA vs. MHCC97H NC: 112.3 ± 11.5 vs. 285.3 ± 11.3, $P < 0.05$; wound assay: HepG2 shA vs. HepG2 NC: 22.83 ± 4.93 vs. 46.31 ± 2.21 μm, $P < 0.05$; wound assay: MHCC97H shA vs. MHCC97H NC: 25.27 ± 0.78 vs. 50.08 ± 3.85 μm, $P < 0.05$). We then analyzed the epithelial-mesenchymal transition (EMT)-associated proteins by Western blotting, which showed that the expressions of vimentin and N-cadherin were decreased in the shA groups than those in the NC groups, although the expressions of E-cadherin were increased [all $P < 0.05$; Figure 3e and 3f].

Silencing *XB130* reduces tumor growth in nude mice and XB130 activates the PI3K/Akt/PTEN pathway

To evaluate the effect of silencing *XB130* on tumorigenesis *in vitro*, we established a nude mouse model of

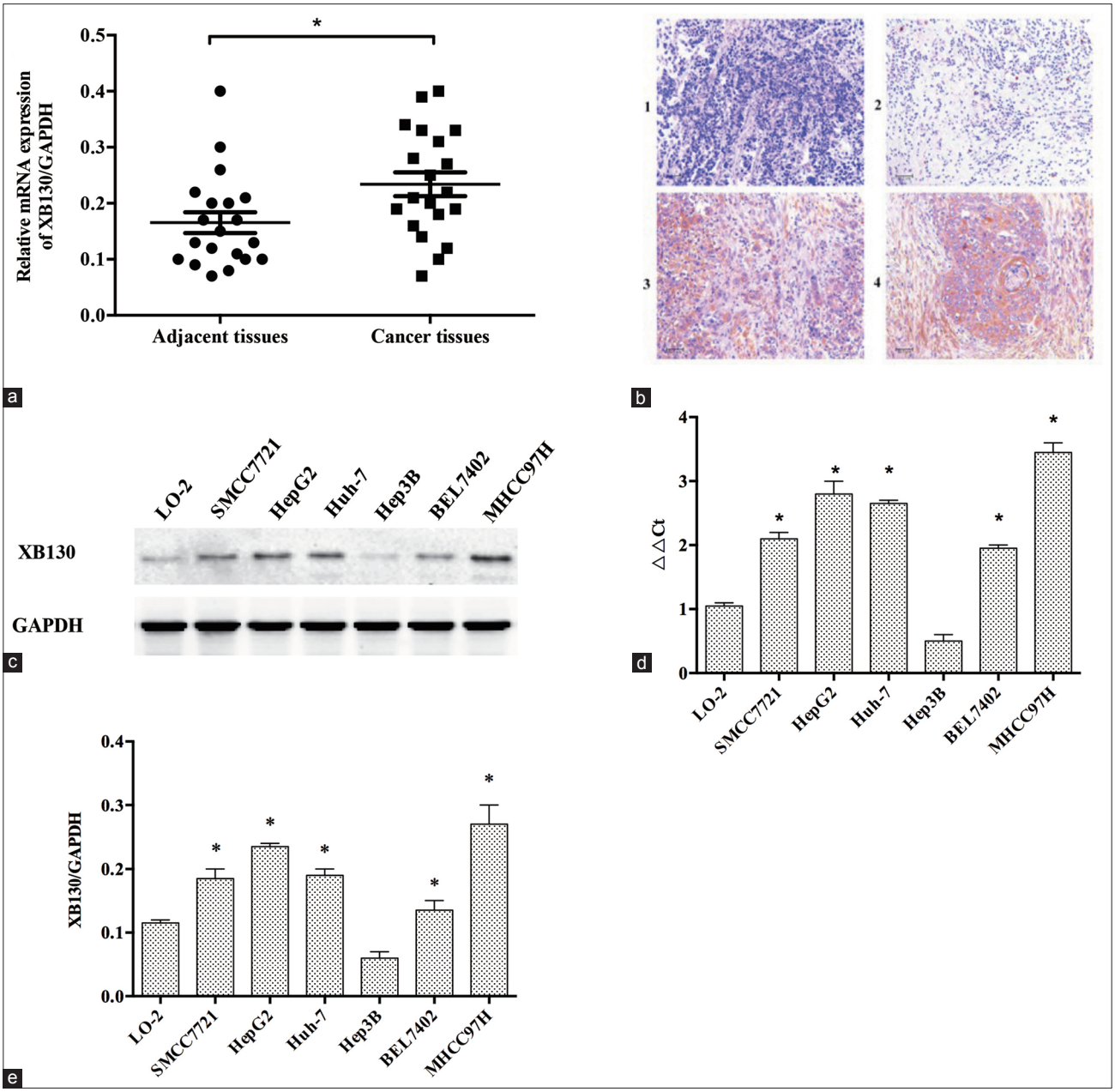

Figure 1: The expression of XB130 in hepatocellular carcinoma tissues and cell lines. (a) The expression of *XB130* in HCC tissues and adjacent tissues measured by qPCR. *$P < 0.05$ versus adjacent tissues. (b) The immunochemistry of XB130 in HCC tissue samples extracted from patients (×200); 1–2: Negative expression; 3–4: Positive expression of XB130. (c) The expression of XB130 in different HCC cells and the normal liver cell line LO-2 measured by qPCR. GAPHD as a loading control, the figure shows the ratio of expression of XB130 to GAPHD. (d) The ratio of each protein to GAPHD. (e) The expression of XB130 in different HCC cells and the normal liver cell line LO-2 measured by Western blotting, with GAPHD as a loading control. *$P < 0.05$ versus LO-2. Data in the bar graphs represent the mean ± standard deviation of three repeated experiments. HCC: Hepatocellular carcinoma; qPCR: Quantitative polymerase chain reaction; GAPHD: Glyceraldehyde-3-phosphate dehydrogenase.

tumor formation and injected the shA and NC groups subcutaneously. We found that subcutaneous tumor formation was significantly lower in the shA group than that in the scramble group [Figure 4a] and that the tumor weight [Figure 4b; HepG2 shA vs. HepG2 NC: 0.59 ± 0.06 g vs. 1.19 ± 0.03 g, $P < 0.05$ and MHCC97H shA vs. MHCC97H NC: 0.70 ± 0.04 g vs. 1.52 ± 0.10 g, $P < 0.05$] and volume [Figure 4c; HepG2 shA vs. HepG2 NC: 977.00 ± 87.00 mm^3 vs. 1819.00 ± 108.14 mm^3, $P < 0.05$ and MHCC97H shA vs. MHCC97H NC: 1377.00 ± 97.86 mm^3 vs. 2354.00 ± 103.66 mm^3, $P < 0.05$] were also significantly lower in the silenced group after 4 weeks. These findings suggest that *XB130* knockdown inhibits the growth of HCC. To investigate the molecular mechanism involved in the cell changes that are induced by a reduction in XB130, we detected changes in related signal pathways by Western blotting [Figure 4d and 4e]. We found that Ser473 (HepG2 shA vs. HepG2 NC: 0.31 ± 0.01 vs. 0.9 ± 0.02 , $P < 0.05$

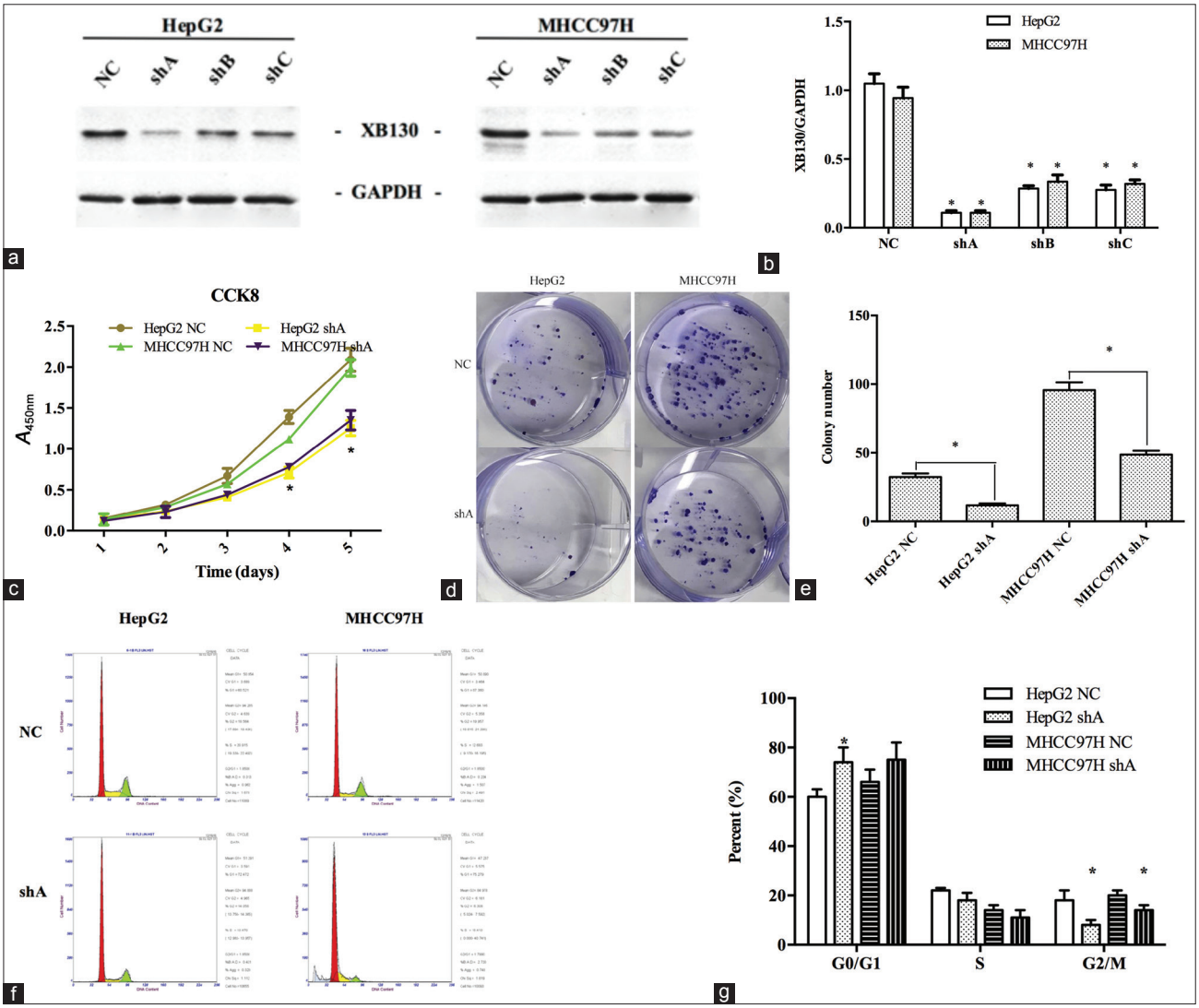

Figure 2: Silencing *XB130* inhibits the proliferation of hepatocellular carcinoma cell lines. (a and b) The expression of XB130 in *XB130*-silenced and scramble (NC) groups measured by Western blotting, with GAPHD as a loading control. There was a significant decrease in XB130 expression of the shA group (*$P < 0.01$ versus NC groups). (c) The viability of cells in various groups measured by a Cell Counting Kit-8 assay. The viability of HepG2 shA and MHCC97H shA was markedly suppressed in a time-dependent manner ($P < 0.05$). (d and e) Clonogenic ability of cells in various groups measured by a colony assay. After silencing *XB130*, the clonogenic ability of HepG2 and MHCC97H cells significantly decreased ($P < 0.05$) compared with the NC group. (f-g) The cell cycle in *XB130*-silenced (shA) and scramble (NC) cells. The cell numbers of G0/G1 phase in HepG2 shA group were higher than HepG2 NC group ($P < 0.05$), and the numbers of G2/M phase in HepG2 shA and MHCC97H shA groups were lower than those in NC groups ($P < 0.05$). *$P < 0.05$ versus NC groups. All detections were repeated three times and the mean values were used for comparison. shA–C: Small hairpin RNA A–C; NC: Scramble small hairpin RNA; GAPHD: Glyceraldehyde-3-phosphate dehydrogenase.

and MHCC97H shA vs. MHCC97H NC: 0.17 ± 0.02 vs. 0.69 ± 0.02, $P < 0.05$), threonine 308 (Thr308; HepG2 shA vs. HepG2 NC: 0.12 ± 0.01 vs. 0.43 ± 0.04, $P < 0.05$ and MHCC97H shA vs. MHCC97H NC: 0.21 ± 0.05 vs. 0.52 ± 0.03, $P < 0.05$), and p-PI3K were significantly lower in HepG2 shA and MHCC97H shA groups (HepG2 shA vs. HepG2 NC: 0.26 ± 0.04 vs. 0.85 ± 0.03, $P < 0.05$ and MHCC97H shA vs. MHCC97H NC: 0.19 ± 0.02 vs. 0.86 ± 0.03, $P < 0.05$), and the level of p-PTEN, which is an inhibitor of p-Akt, was upregulated (HepG2 shA vs. HepG2 NC: 0.42 ± 0.04 vs. 0.25 ± 0.05, $P < 0.05$ and MHCC97H shA vs. MHCC97H NC: 0.26 ± 0.02 vs. 0.14 ± 0.01, $P < 0.05$), whereas there was no change in the levels of Akt, PTEN, and PI3K. Thus, we confirmed that XB130 activates the PI3K/Akt/PTEN pathway.

Knockdown of *XB130* sensitizes hepatocellular carcinoma to TRAIL-induced apoptosis

Then, we explored the effect of silencing *XB130* on the apoptosis of HCC cell lines using flow cytometry assay and caspase assay. We found that the apoptosis of shA groups was increased significantly compared with that of NC groups, and caspase-3, -8, and -9 were also increased ($P < 0.05$). A study showed that activating the PI3K/Akt pathway contributed to tolerance to tumor necrosis factor (TNF)-related apoptosis-inducing ligand (TRAIL).[20] We found that when

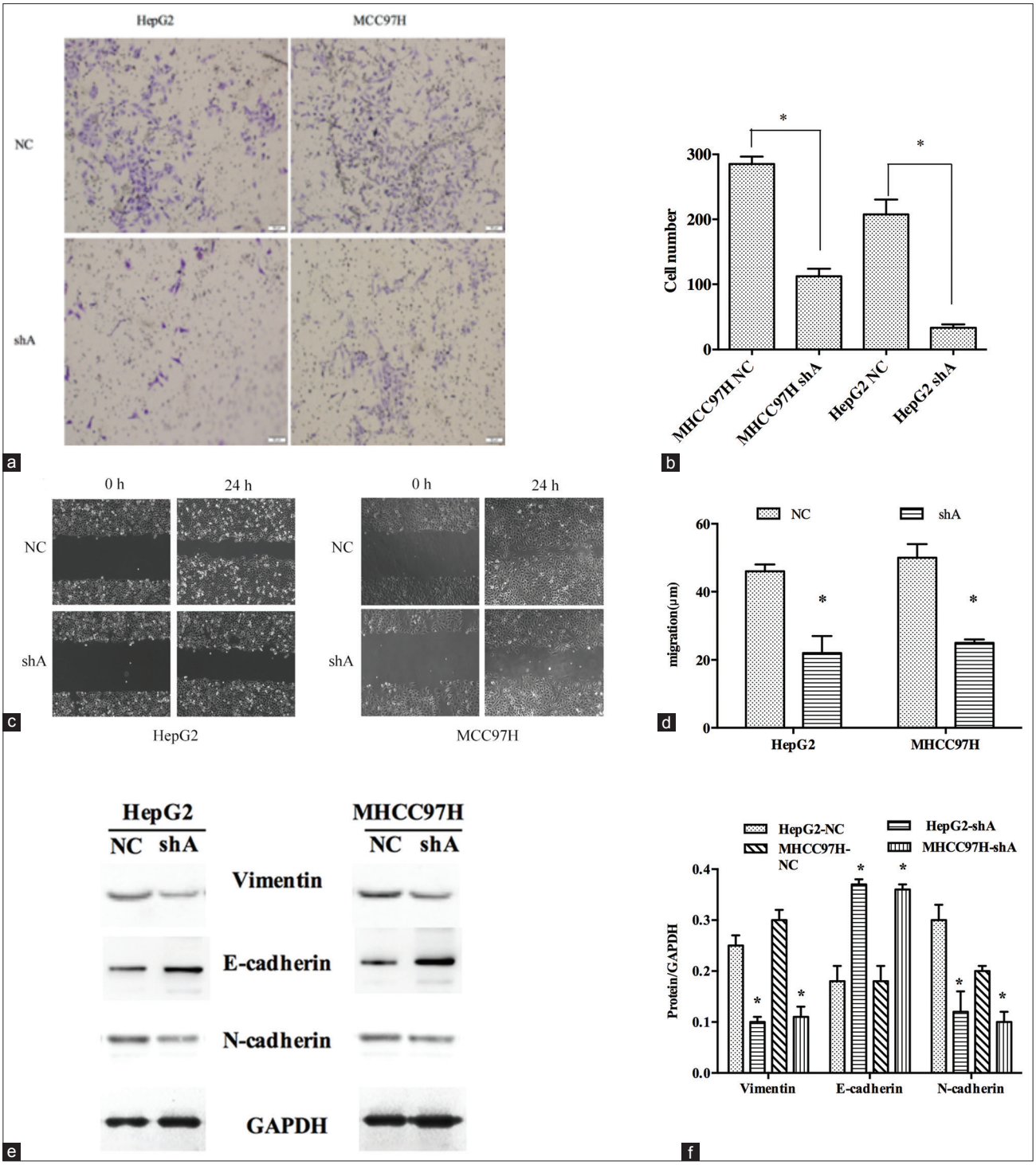

Figure 3: Silencing *XB130* inhibits the motility and invasiveness of hepatocellular carcinoma cell lines and alters epithelial-mesenchymal transition markers. (a and b) Cell migration as indicated by a Transwell migration assay. The number of cells migrating into the lower chamber was significantly lower in the shA groups than that in the NC groups (*$P < 0.01$). (c and d) Results of a wound healing assay. Reduced cell migration was observed in the shA groups ($P < 0.05$). (e) The expression of epithelial-mesenchymal transition-related markers measured by Western blotting. (f) The ratio of each protein to GAPDH. Compared to the NC groups, the expressions of vimentin and N-cadherin were decreased, while the expression of E-cadherin was increased ($P < 0.05$). Original magnification of (a) and (c), ×200. *$P < 0.05$ versus NC groups. All detections were repeated three times and the mean values were used for comparison. shA: Small hairpin RNA A; NC: Scramble small hairpin RNA; GAPHD: Glyceraldehyde-3-phosphate dehydrogenase.

cells were incubated with TRAIL (100 ng/ml) using dimethyl sulfoxide (DMSO) as a control, the apoptosis of HepG2 NC and MHCC97H NC did not change, although apoptosis increased in shA + TRAIL groups compared with that in NC + TRAIL and shA + DMSO groups [$P < 0.05$; Figure 5a and 5b]. The activities of caspase-3, -8, and -9 increased in HepG2 shA + TRAIL and MHCC97H shA + TRAIL groups [$P < 0.05$; Figure 5c-5e], indicating that XB130 can

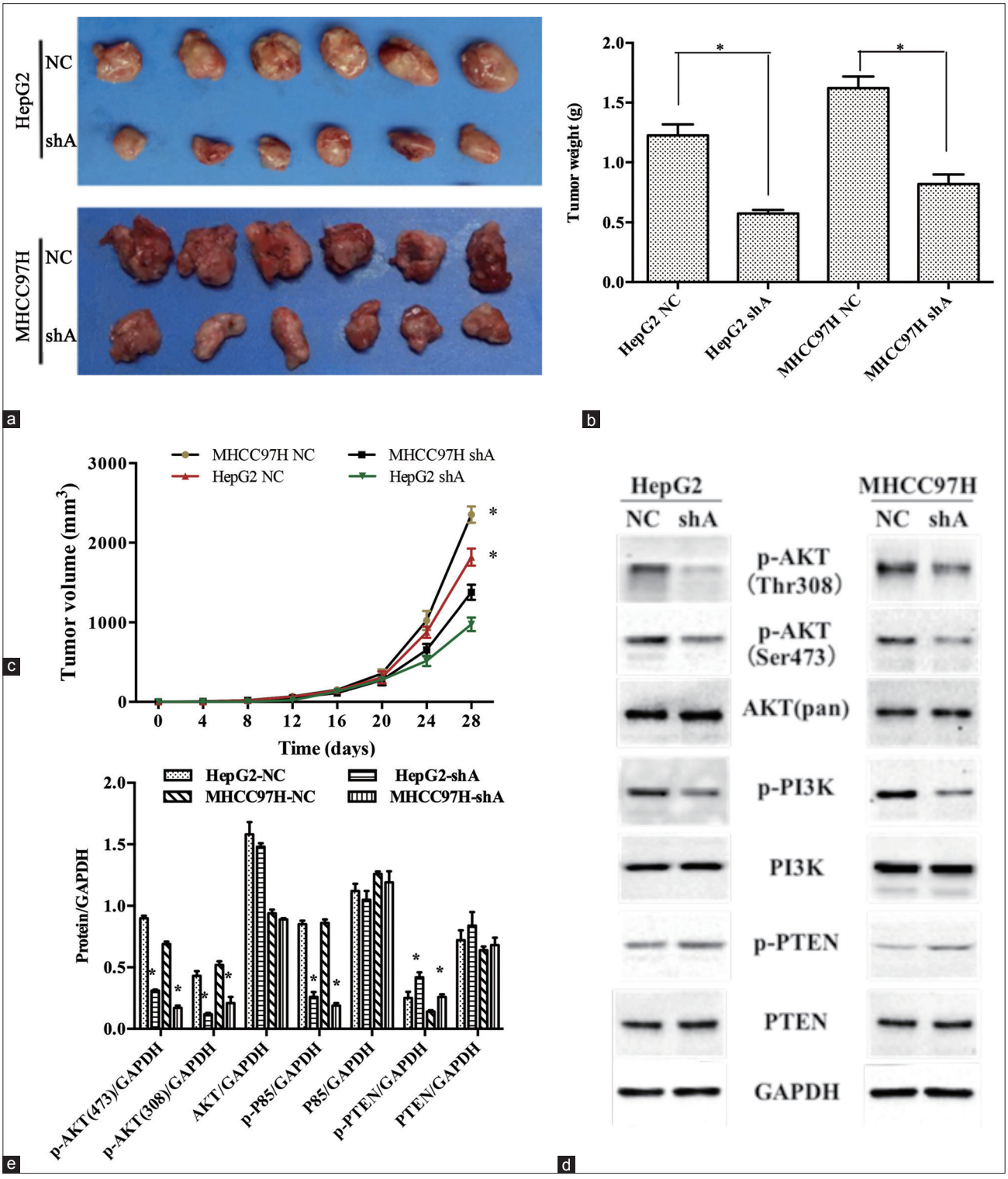

Figure 4: Silencing *XB130* reduces tumor growth in nude mice and XB130 activates the PI3K/Akt/PTEN pathway. (a) Tumor volume following the subcutaneous injection of cells into the right posterior flank regions of mice. The tumor volume was smaller in the *XB130*-silenced (HepG2 shA and MHCC97H shA) group than that in the scramble group. (b) Tumor weight following the injection of nude mice with shA or NC cells. The results showed that the weight in shA groups was lower than that in NC groups (*$P < 0.05$). (c) A growth curve for tumors following the injection of nude mice with HepG2 shA, HepG2 NC, MHCC97H shA, or MHCC97H NC cells. The results confirmed that tumor volume of shA groups was smaller than that in NC groups. (d) The expressions of Akt, Ser-473, PI3K, p-PI3K, PTEN, phosphorylated PTEN, and Thr308 were examined by Western blotting. (e) The ratio of each protein to GAPHD. The levels of p-Akt, p-PI3K, p-PTEN, and Thr308 were lower in the *XB130*-silenced groups than those in the scramble groups, while there was no difference in the levels of Akt, PI3K, and PTEN. *$P < 0.05$ versus NC groups. Data in the bar graphs represent the mean ± standard deviation of three repeated experiments. shA: Small hairpin RNA A; NC: Scramble small hairpin RNA; p-: Phosphorylated; Akt: Protein kinase B; Ser: Serine; PI3K: Phosphoinositide 3-kinase; PTEN: Phosphatase and tensin homolog; Thr308: Threonine 308; GAPHD: Glyceraldehyde-3-phosphate dehydrogenase.

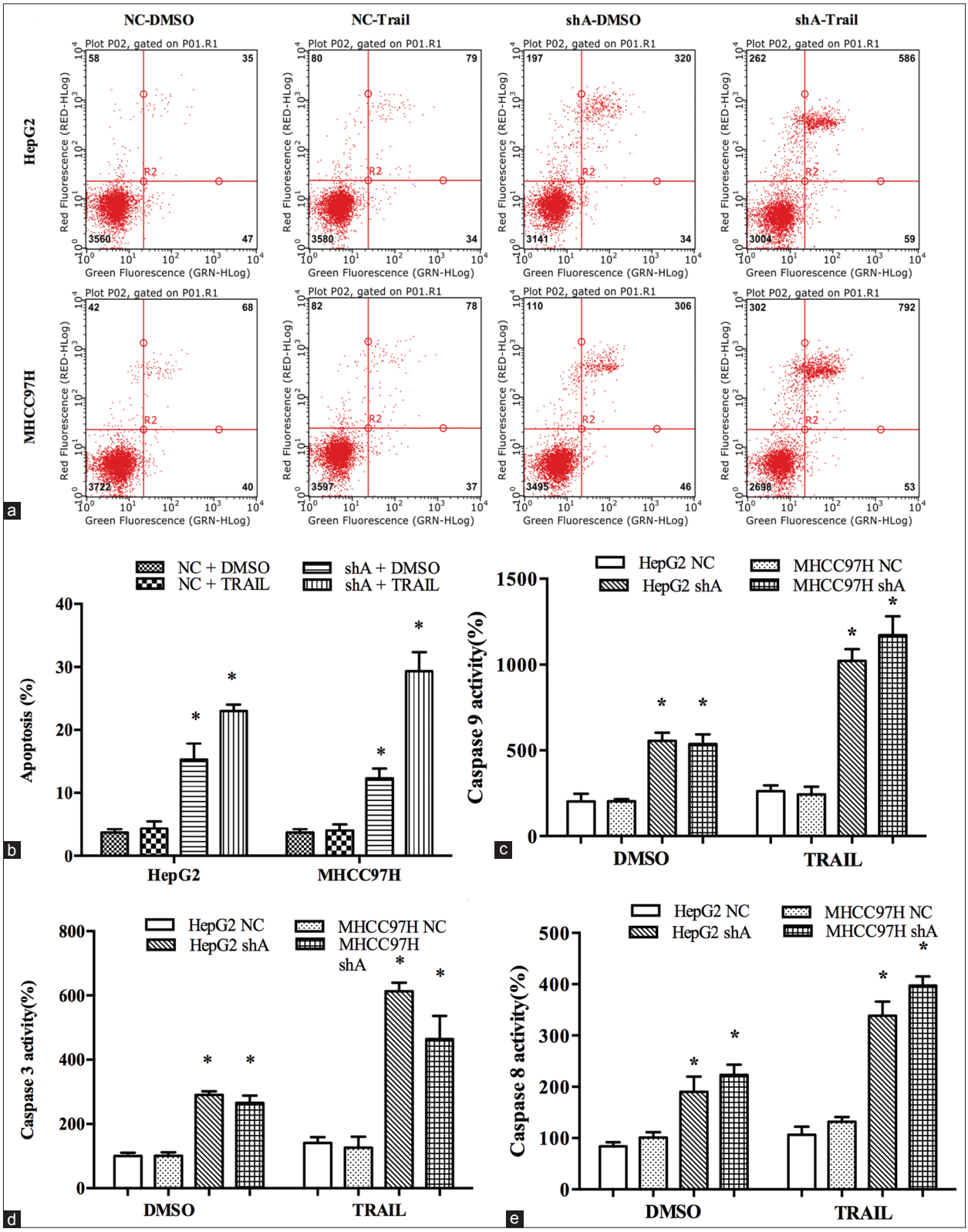

Figure 5: Downregulation of XB130 sensitizes hepatocellular carcinoma cells to TRAIL-induced apoptosis. (a and b) The apoptosis of four different cell lines (HepG2 shA, HepG2 NC, MHCC97H shA, and MHCC97H NC) treated with 100 ng/ml TRAIL for 24 h and measured by Annexin V, DMSO as a control. HepG2 NC and MHCC97H NC were tolerant to TRAIL, and apoptosis was obviously increased in shA groups when the cells were treated with TRAIL compared with the NC group (*$P < 0.01$). (c-e) Caspase 3, caspase 8, and caspase 9 activities were determined fluorometrically in cell extracts using Ac-DEVD-AMC, Ac-IETD-AFC, and Ac-LEHD-AMC as fluorogenic substrate, respectively. And, the caspase-3, caspase-8, and caspase-9 activities were significantly increased in shA/TRAIL groups compared to other groups. *$P < 0.05$ versus NC groups. All of the experiments were repeated three times. Data in the bar graphs represent the mean ± standard deviation of three repeated experiments. shA: Small hairpin RNA A; NC: Scramble small hairpin RNA; DMSO: Dimethyl sulfoxide; TRAIL: Tumor necrosis factor-related apoptosis-inducing ligand.

contribute to tolerance of HCC to TRAIL by activating the PI3K/Akt pathway.

Discussion

XB130 is a newly discovered adaptor protein that plays a critical role in the regulation of signal transduction, affecting cell proliferation, survival, invasion, and metastasis.[13,15,21] Few studies have investigated the relationship between XB130 and tumor development to date, and it has been shown that XB130 can be used as a predictor of tumorigenesis in a variety of tumors, although its relationship with the clinical stage and prognosis differs among tumor types. For instance, Chen *et al*.[15] found that the positive expression rate of XB130 in prostate cancer tissues was 85.6% by immunohistochemistry and that this high expression of XB130 was positively correlated with the high expression of PSA, PAP, tumor size, and T grade, thus indicating a poor prognosis. Similarly, Shiozaki *et al*.[13] found that the positive expression rate of XB130 in esophageal cancer tissues was 71.2% and confirmed this high expression in an esophageal cancer cell line by Western blotting. Consistent with this, the overexpression of XB130 has been found in pancreatic ductal adenocarcinoma,[22] breast cancer,[23] and cartilage cancer[24] and is associated with a short survival time. However, XB130 plays a different role in gastric cancer, with Shi *et al*.[18] demonstrating that although XB130 could be used as a predictor for gastric cancer due to its high expression in cancer tissues from 411 patients with gastric cancer by immunohistochemistry, a low expression of XB130 predicted a poor prognosis, and there was a negative correlation between the expression of XB130 and the sensitivity to 5-FU in the gastric cancer cell line SGC7901. In HCC tissues, Zuo *et al*.[19] found that the positive expression rate of XB130 was 75% through the analysis of 64 HCC cases by immunohistochemistry and that XB130 was not related to the clinical stage, TNM, or prognosis. In the present study, we found that the expression of XB130 was higher in HCC tissues than that in adjacent nontumor tissues through the analysis of 20 pairs of HCC tissues by quantitative qRT-PCR, and the positive expression rate was 80% in HCC tissues by immunohistochemistry, although it was only 20% in the adjacent nontumor tissues. However, it was difficult to explore the relationship between the expression of XB130 and clinical classification and prognosis due to the limited number of cases; this needs further validation. We also found that XB130 was highly expressed in hepatocarcinoma cell lines by quantitative PCR and Western blotting, demonstrating that XB130 may be used as an indicator in the clinical diagnosis of HCC.

Tumor development and progression is a complex process that involves multiple factors, multigene changes, and multistep evolution.[25] Abnormal levels of proliferation, migration, invasive growth, and metastatic potential are the fundamental characteristics that make malignant tumor cells different from benign tumor cells. Thus, knowledge of the molecular mechanism of tumor development brings hope pertaining to finding a cure for malignant tumors.[26] It has previously been demonstrated that XB130 is associated with tumor proliferation, migration, and invasion.[27] Shiozaki *et al*.[13] found that silencing *XB130* arrested thyroid cancer WRO cells in the G0/G1 phase, although the number of S phase cells and levels of the proliferation-associated proteins Ki-67 and proliferating cell nuclear antigen decreased, as did the tumorigenicity of tumor cells *in vitro*. Gene analysis[21] has also revealed that the expression of 246 types of genes changed following the downregulation of XB130; 57 of these genes are related to cell proliferation, survival, and cycle-related pathways, and pathway analysis showed that XB130 is most strongly related to cancer and that it may affect cell proliferation, growth, and cycle. Shi *et al*.[16] also found similar results in gastric cancer, wherein the knockdown of *XB130* in SGC7901 and MNK45 cells led to a decrease in cell proliferation, an increase in G0/G1 phase, and a decrease in S phase cells. In addition, Western blotting showed that the expressions of E-cadherin, α-catenin, and β-catenin in EMT were significantly increased, although those of the invasion-related proteins MMP-2, MMP-9, and CD44, as well as p-Akt/Akt, were decreased, indicating that the downregulation of XB130 inhibits the PI3K/Akt pathway. In the present study, we found that the downregulation of XB130 in HepG2 and MHCC97H cells impaired cell proliferation, increased the number of tumor cells in the G0/G1 phase, decreased the number of cells in the G2/M phase, and suppressed tumor formation in nude mice. Thus, XB130 may be used as a new target for the treatment of HCC.

Abnormal activation of the PI3K/Akt pathway is closely related to tumor development; activated PI3K converts PIP2 to PIP3, which acts as a second messenger to activate a number of signaling molecules downstream of the signal pathway involved in cell proliferation, differentiation, apoptosis, survival, and migration.[28-30] There are three types of PI3K family in mammals: the type I PI3K and its downstream molecular serine/threonine protein kinase make up a signaling pathway (PI3K/Akt), which is closely related to tumor development.[31] Type-IA PI3K is a heterodimer comprising P85 regulatory subunit and P110 catalytic subunit. P85 regulatory subunits include P85α, P85β, and P85γ, and P85α is the most regulated subunit.[28] XB130 is a tyrosine kinase substrate that can phosphorylate tyrosine by interacting with other tyrosine kinases at the SH2 and SH3 domains of the N-terminal of Src. It has been shown that SH2 on XB130 has a YxxM modification site and that its specific binding to the p85α subunit of PI3K activates the Akt pathway,[17] whereas a reduction in XB130 can affect multiple molecules downstream of Akt.[15] Akt is a serine/threonine kinase, also known as protein kinase B, which is highly homologous to protein kinase A and protein kinase C, is one of the major downstream effector molecules of PI3K, and can directly phosphorylate many transcriptional factors; its activation requires the activation of Thr308 and Ser473.[32] Consistent with this, in the present study, we found that a reduction in XB130 can regulate the expression of the

Akt-related phosphorylation markers Ser473 and Thr308 and inhibit the phosphorylation of PI3K but had no effect on the total levels of Akt and PI3K. PTEN gene can inhibit cell carcinogenesis by the negative regulation of PI3K/Akt. In normal cells, PTEN has phosphatase activity, which can make PIP3 dephosphoric acid to PIP2 to lose the messenger function and thereby inhibit the PI3K/Akt signaling pathway, leading to apoptosis and inhibition of proliferation.[33] In contrast, the mutations or deletions of PTEN will lose normal inhibition of PIP2 conversion to PIP3, increasing intracellular PIP3 accumulation and Akt activation, thereby inhibiting apoptosis, promoting cell growth, and stimulating tumor angiogenesis.[34] In our study, we confirmed that reduction of XB130 can increase the level of p-PTEN, but the total level of PTEN does not change. Thus, we conclude that XB130 may activate PI3K/Akt to maintain tumor cell proliferation, invasion, and metastasis.

EMT is also an important biological process for the migration and invasion of epithelial cell-derived malignant cells[35] and is strongly associated with the PI3K/Akt pathway.[36,37] The expression of E-cadherin, β-cadherin, and vimentin in mesenchymal tissue can be upregulated by Akt. We used Western blotting to detect EMT-related markers, which showed that downregulation of XB130 upregulated E-cadherin expression, although downregulation of N-cadherin and vimentin could inhibit the progression of EMT and affect the invasion and metastasis of HCC. Thus, it appears that XB130 can promote EMT of HCC through activation of the PI3K/Akt pathway.

TRAIL is a member of the TNF superfamily that can induce tumor cell apoptosis through binding with its receptor. The fact that TRAIL can kill tumor cells but is nontoxic to normal cells, which are different from TNF and Fas, has attracted the attention of many scientists.[38-40] Some studies confirmed that many tumor cells are resistant to TRAIL, including HCC cells.[41,42] It has previously been shown that activation of the PI3K/Akt pathway promotes tumor cell tolerance to TRAIL, whereas inhibition of this pathway can make tumor cells susceptible to TRAIL.[20] Because reduction of XB130 can inhibit the activation of PI3K/Akt, we explored whether XB130 contributes to the resistance to TRAIL by HCC. Our study confirmed that a reduction in XB130 and incubation with TRAIL can significantly increase tumor cell apoptosis, suggesting that downregulation of XB130 can sensitize liver cancer cells to TRAIL-induced apoptosis. Although there are many factors contributing TRAIL resistance,[43,44] including decoy receptor, c-FLIP, nuclear factor-κB, and activation of anti-apoptotic kinase signaling, whether the sensitivity of HCC cells to TRAIL increases only by inhibiting the PI3K/Akt pathway still needs further validation.

In summary, we confirmed the high expression of XB130 in HCC tissues and cell lines and showed that downregulation of XB130 can affect the proliferation, migration, and invasiveness of HCC cells, arresting them in the G0/G1 phase and inhibiting EMT-related processes. Furthermore, a reduction in XB130 can increase the sensitivity of HCC cells to TRAIL-induced apoptosis, which might provide a theoretical basis for the clinical treatment of liver cancer. However, the expression of XB130 in Hep3B was higher than that in normal liver cell line, the mechanism may be different from others, which also needs further study.

Financial support and sponsorship

This work was supported by grants from the Beijing Municipal Administration of Hospital Clinical Medicine Development of Special Funding Support (No. ZYLX201612), the Capital Foundation of Medical Development (No. shoufa2016-2-2053), and the Beijing Tongren Hospital Funds (No. TRYY-KYJJ-2015-032).

Conflicts of interest

There are no conflicts of interest.

References

1. Marquardt JU, Thorgeirsson SS. SnapShot: Hepatocellular carcinoma. Cancer Cell 2014;25:550.e1. doi: 10.1016/j.ccr.2014.04.002.
2. Siegel R, Naishadham D, Jemal A. Cancer statistics, 2012. CA Cancer J Clin 2012;62:10-29. doi: 10.3322/caac.20138.
3. Llovet JM, Burroughs A, Bruix J. Hepatocellular carcinoma. Lancet 2003;362:1907-17. doi: 10.1016/s0140-6736(03)14964-1.
4. Avila MA, Berasain C, Sangro B, Prieto J. New therapies for hepatocellular carcinoma. Oncogene 2006;25:3866-84. doi: 10.1038/sj.onc.1209550.
5. Xu J, Bai XH, Lodyga M, Han B, Xiao H, Keshavjee S, *et al.* XB130, a novel adaptor protein for signal transduction. J Biol Chem 2007;282:16401-12. doi: 10.1074/jbc.M701684200.
6. Alexandropoulos K, Baltimore D. Coordinate activation of c-src by SH3 – And SH2-binding sites on a novel p130Cas-related protein, sin. Genes Dev 1996;10:1341-55. doi: 10.1101/gad.10.11.1341.
7. Zhu Q, Youn H, Tang J, Tawfik O, Dennis K, Terranova PF, *et al.* Phosphoinositide 3-OH kinase p85alpha and p110beta are essential for androgen receptor transactivation and tumor progression in prostate cancers. Oncogene 2008;27:4569-79. doi: 10.1038/onc.2008.91.
8. Courtneidge SA. Role of src in signal transduction pathways. The Jubilee Lecture. Biochem Soc Trans 2002;30:11-7. doi: 10.1042/bst0300011.
9. Xing L, Ge C, Zeltser R, Maskevitch G, Mayer BJ, Alexandropoulos K, *et al.* C-src signaling induced by the adapters sin and cas is mediated by rap1 GTPase. Mol Cell Biol 2000;20:7363-77. doi: 10.1128/MCB.20.19.7363-7377.2000.
10. Okutani D, Lodyga M, Han B, Liu M. Src protein tyrosine kinase family and acute inflammatory responses. Am J Physiol Lung Cell Mol Physiol 2006;291:L129-41. doi: 10.1152/ajplung.00261.2005.
11. Lodyga M, De Falco V, Bai XH, Kapus A, Melillo RM, Santoro M, *et al.* XB130, a tissue-specific adaptor protein that couples the RET/PTC oncogenic kinase to PI 3-kinase pathway. Oncogene 2009;28:937-49. doi: 10.1038/onc.2008.447.
12. Shiozaki A, Liu M. Roles of XB130, a novel adaptor protein, in cancer. J Clin Bioinforma 2011;1:10. doi: 10.1186/2043-9113-1-10.
13. Shiozaki A, Shen-Tu G, Bai X, Iitaka D, De Falco V, Santoro M, *et al.* XB130 mediates cancer cell proliferation and survival through multiple signaling events downstream of Akt. PLoS One 2012;7:e43646. doi: 10.1371/journal.pone.0043646.
14. Shiozaki A, Kosuga T, Ichikawa D, Komatsu S, Fujiwara H, Okamoto K, *et al.* XB130 as an independent prognostic factor in human esophageal squamous cell carcinoma. Ann Surg Oncol 2013;20:3140-50. doi: 10.1245/s10434-012-2474-4.
15. Chen B, Liao M, Wei Q, Liu F, Zeng Q, Wang W, *et al.* XB130 is overexpressed in prostate cancer and involved in cell growth and invasion. Oncotarget 2016;7:59377-87. doi: 10.18632/oncotarget.11074.

16. Shi M, Zheng D, Sun L, Wang L, Lin L, Wu Y, *et al.* XB130 promotes proliferation and invasion of gastric cancer cells. J Transl Med 2014;12:1. doi: 10.1186/1479-5876-12-1.
17. Shiozaki A, Lodyga M, Bai XH, Nadesalingam J, Oyaizu T, Winer D, *et al.* XB130, a novel adaptor protein, promotes thyroid tumor growth. Am J Pathol 2011;178:391-401. doi: 10.1016/j.ajpath.2010.11.024.
18. Shi M, Huang W, Lin L, Zheng D, Zuo Q, Wang L, *et al.* Silencing of XB130 is associated with both the prognosis and chemosensitivity of gastric cancer. PLoS One 2012;7:e41660. doi: 10.1371/journal.pone.0041660.
19. Zuo Q, Huang H, Shi M, Zhang F, Sun J, Bin J, *et al.* Multivariate analysis of several molecular markers and clinicopathological features in postoperative prognosis of hepatocellular carcinoma. Anat Rec (Hoboken) 2012;295:423-31. doi: 10.1002/ar.21531.
20. Feng X, Jiang J, Shi S, Xie H, Zhou L, Zheng S, *et al.* Knockdown of miR-25 increases the sensitivity of liver cancer stem cells to TRAIL-induced apoptosis via PTEN/PI3K/Akt/Bad signaling pathway. Int J Oncol 2016;49:2600-10. doi: 10.3892/ijo.2016.3751.
21. Takeshita H, Shiozaki A, Bai XH, Iitaka D, Kim H, Yang BB, *et al.* XB130, a new adaptor protein, regulates expression of tumor suppressive microRNAs in cancer cells. PLoS One 2013;8:e59057. doi: 10.1371/journal.pone.0059057.
22. Zhang J, Jiang X, Zhang J. Prognostic significance of XB130 expression in surgically resected pancreatic ductal adenocarcinoma. World J Surg Oncol 2014;12:49. doi: 10.1186/1477-7819-12-49.
23. Li J, Sun W, Wei H, Wang X, Li H, Yi Z, *et al.* Expression of XB130 in human ductal breast cancer. Int J Clin Exp Pathol 2015;8:5300-8.
24. Wang X, Wang R, Liu Z, Hao F, Huang H, Guo W, *et al.* XB130 expression in human osteosarcoma: A clinical and experimental study. Int J Clin Exp Pathol 2015;8:2565-73.
25. Mareel M, Leroy A. Clinical, cellular, and molecular aspects of cancer invasion. Physiol Rev 2003;83:337-76. doi: 10.1152/physrev.00024.2002.
26. Naito S, von Eschenbach AC, Giavazzi R, Fidler IJ. Growth and metastasis of tumor cells isolated from a human renal cell carcinoma implanted into different organs of nude mice. Cancer Res 1986;46:4109-15.
27. Bai XH, Cho HR, Moodley S, Liu M. XB130-A novel adaptor protein: Gene, function, and roles in tumorigenesis. Scientifica (Cairo) 2014;2014:903014. doi: 10.1155/2014/903014.
28. Katso R, Okkenhaug K, Ahmadi K, White S, Timms J, Waterfield MD, *et al.* Cellular function of phosphoinositide 3-kinases: Implications for development, homeostasis, and cancer. Annu Rev Cell Dev Biol 2001;17:615-75. doi: 10.1146/annurev.cellbio.17.1.615.
29. Wang Q, Yu WN, Chen X, Peng XD, Jeon SM, Birnbaum MJ, *et al.* Spontaneous hepatocellular carcinoma after the combined deletion of Akt isoforms. Cancer Cell 2016;29:523-35. doi: 10.1016/j.ccell.2016.02.008.
30. Jiang H, Fan D, Zhou G, Li X, Deng H. Phosphatidylinositol 3-kinase inhibitor (LY294002) induces apoptosis of human nasopharyngeal carcinoma *in vitro* and *in vivo*. J Exp Clin Cancer Res 2010;29:34. doi: 10.1186/1756-9966-29-34.
31. Fortin J, Mak TW. Targeting PI3K signaling in cancer: A cautionary tale of two AKTs. Cancer Cell 2016;29:429-31. doi: 10.1016/j.ccell.2016.03.020.
32. Cicenas J. The potential role of Akt phosphorylation in human cancers. Int J Biol Markers 2008;23:1-9.
33. Carnero A, Blanco-Aparicio C, Renner O, Link W, Leal JF. The PTEN/PI3K/AKT signalling pathway in cancer, therapeutic implications. Curr Cancer Drug Targets 2008;8:187-98. doi: 10.2174/156800908784293659.
34. Wise HM, Hermida MA, Leslie NR. Prostate cancer, PI3K, PTEN and prognosis. Clin Sci (Lond) 2017;131:197-210. doi: 10.1042/cs20160026.
35. De Craene B, Berx G. Regulatory networks defining EMT during cancer initiation and progression. Nat Rev Cancer 2013;13:97-110. doi: 10.1038/nrc3447.
36. Wen W, Ding J, Sun W, Fu J, Chen Y, Wu K, *et al.* Cyclin G1-mediated epithelial-mesenchymal transition via phosphoinositide 3-kinase/Akt signaling facilitates liver cancer progression. Hepatology 2012;55:1787-98. doi: 10.1002/hep.25596.
37. Xue G, Restuccia DF, Lan Q, Hynx D, Dirnhofer S, Hess D, *et al.* Akt/PKB-mediated phosphorylation of Twist1 promotes tumor metastasis via mediating cross-talk between PI3K/Akt and TGF-β signaling axes. Cancer Discov 2012;2:248-59. doi: 10.1158/2159-8290.cd-11-0270.
38. Wiley SR, Schooley K, Smolak PJ, Din WS, Huang CP, Nicholl JK, *et al*. Identification and characterization of a new member of the TNF family that induces apoptosis. Immunity 1995;3:673-82.
39. Pitti RM, Marsters SA, Ruppert S, Donahue CJ, Moore A, Ashkenazi A, *et al.* Induction of apoptosis by Apo-2 ligand, a new member of the tumor necrosis factor cytokine family. J Biol Chem 1996;271:12687-90. doi: 10.1074/jbc.271.22.12687.
40. Hall MA, Cleveland JL. Clearing the TRAIL for cancer therapy. Cancer Cell 2007;12:4-6. doi: 10.1016/j.ccr.2007.06.011.
41. Wang G, Zhan Y, Wang H, Li W. ABT-263 sensitizes TRAIL-resistant hepatocarcinoma cells by downregulating the bcl-2 family of anti-apoptotic protein. Cancer Chemother Pharmacol 2012;69:799-805. doi: 10.1007/s00280-011-1763-0.
42. Liang C, Xu Y, Li G, Zhao T, Xia F, Li G, *et al.* Downregulation of DcR3 sensitizes hepatocellular carcinoma cells to TRAIL-induced apoptosis. Onco Targets Ther 2017;10:417-28. doi: 10.2147/ott.s127202.
43. Lim B, Allen JE, Prabhu VV, Talekar MK, Finnberg NK, El-Deiry WS, *et al.* Targeting TRAIL in the treatment of cancer: New developments. Expert Opin Ther Targets 2015;19:1171-85. doi: 10.1517/14728222.2015.1049838.
44. Wang F, Lin J, Xu R. The molecular mechanisms of TRAIL resistance in cancer cells: Help in designing new drugs. Curr Pharm Des 2014;20:6714-22. doi: 10.2174/1381612820666140929100735.

*XB130*敲除抑制肝细胞癌细胞的增殖、侵袭以及转移，并使其对TRAIL诱导的细胞凋亡敏感

摘要

背景：XB130是新近发现的一种在许多恶性肿瘤中高表达的衔接蛋白，但很少有研究表明研究了它在肝细胞癌（HCC）中的作用。因此，本研究探讨了这XB130与肝癌之间的关系并研究其分子作用机制。

方法：采用RT-PCR、免疫组化及蛋白印迹法比较HCC组织与癌旁组织中XB130的表达，并通过shRNA 将*XB130*沉默。并通过克隆形成实验、划痕实验、集落形成实验及流式细胞术观察其对肝癌细胞系增殖、侵袭、转移及细胞周期的影响。

结果：我们发现XB130在HCC组织中高表达（癌组织与邻近组织：0.23±0.02比0.17±0.02，P<0.05），肝癌细胞系中MHCC97H和HepG2表达最高（MHCC97H和HepG2与正常肝细胞系LO-2：分别为2.35±0.26和2.04±0.04比1.00±0.04，均P<0.05）。CCK-8实验和裸鼠成瘤实验显示，沉默*XB130*在体内和体外都能抑制细胞增殖能力，流式细胞术检测证明沉默*XB130*后可以使肝癌细胞在HepG2的G0 / G1期停滞（HepG2 XB130 [shA]与HepG2 [NA]：74.32±5.86％ 比 60.21±3.07％，P<0.05），G2 / M期细胞数减少（HepG2 shA 比HepG2 NA：8.06±2.41％比18.36±4.42％，P<0.05）。此外，细胞侵袭转移能力受到损害，且上皮 - 间质转化相关指标波形蛋白和N-钙粘蛋白表达下调，E-钙粘蛋白水平上调。 Western blotting显示磷酸化磷酸肌醇3-激酶（PI3K）水平和磷酸化蛋白激酶B（p-Akt）也增加，表明XB130激活了PI3K / Akt通路。此外，我们发现XB130的减少增加了肝癌细胞系对肿瘤坏死因子相关凋亡诱导配体诱导的细胞凋亡的敏感性。

结论：我们的研究结果表明，XB130不仅可以用作肝癌的预测因子，还可以作为肝癌的治疗靶点之一。